

Phosphorus-containing polyhedral oligomeric silsesquioxane/polyimides hybrid materials with low dielectric constant and low coefficients of thermal expansion

Xuesong Li,¹ Jinmeng Hao,¹ Qiyang Jiang,¹ Jianxin Mu,¹ Zhenhua Jiang²

¹College of Chemistry, Key Laboratory (B) of Super Engineering Plastics, Ministry of Education, Jilin University, Changchun, PR China

²Alan G. MacDiarmid Lab, College of Chemistry, Jilin University, Changchun, PR China

Correspondence to: J. Mu (E-mail: jianxin_mu@jlu.edu.cn)

ABSTRACT: Novel phosphorus-containing polyhedral oligomeric silsesquioxane (POSS)/polyimides (PI) hybrid materials with low dielectric constant and low linear coefficients of thermal expansion (CTE) were prepared and characterized. The POSS/PI hybrid materials were synthesized with octa(aminopropyl)silsesquioxane (OAPS) and a series of phosphorus-containing polyamide acids (PAA). The PAAs were synthesized with bis(4-aminophenoxy) phenyl phosphine oxide (BAPPO), 4,4'-diaminodiphenyl ether (ODA) and 3,3',4,4'-biphenyl tetracarboxylic dianhydride (BPDA). The structures and properties of the hybrid materials were characterized. And the effect of the phosphorus-containing structure on the POSS/PI hybrid materials was discussed. The dielectric constants and CTE of the hybrid materials were remarkably lower than that of the unmodified POSS/PI films. The lowest values of dielectric constant and CTE could achieve as low as 2.64 (1 MHz) and 27.45 ppm/K. Besides, the hybrid materials also had excellent thermal properties. The highest 5% weight loss temperature of the hybrid materials was as high as 580°C under air. © 2015 Wiley Periodicals, Inc. *J. Appl. Polym. Sci.* **2015**, *132*, 42611.

KEYWORDS: dielectric properties; polyimides; structure–property relations

Received 30 June 2015; accepted 11 June 2015

DOI: 10.1002/app.42611

INTRODUCTION

With the rapid development of the ultralarge-scale integration, the continuing miniaturization of feature device sizes in integrated circuits industry toward nanometer scale urgently cast an increasing demand on low dielectric constant materials.¹ As high-performance low dielectric constant materials, aromatic polyimides (PIs) had been widely studied in academic and industrial fields and actually applied to a variety of electric, microelectronic, and optoelectronic devices for their reliable and excellent properties, i.e., considerably high glass transition temperatures (T_g) overcoming the solder-reflowing processes, high resistance to chemicals, good dielectric, and mechanical properties.^{2–5} However, even such superior properties of conventional aromatic PI systems were still unable to satisfy the rapid development of the electronic device technologies. The market demand of polyimides with not only low dielectric constants and good thermal properties, but also low CTE had also increased.^{6–12}

Polyhedral oligomeric silsesquioxanes (POSS) due to their excellent properties received extensive attention for preparation of high-performance low dielectric constant materials. POSS was a cube-octameric molecule with an inner inorganic silicon and

oxygen framework which was covered externally by organic substituents. It had a nanometer-sized cage structure and can be functionalized with various organic groups.^{13–17} Because of the nanometer structure of POSS the introduction of POSS into polyimides can not only enhance thermal properties, but also reduce the dielectric constant and linear coefficients of thermal expansion of PI films. POSS/PI hybrid materials with enhanced thermal stability and thermo-dimensional stability had been reported by Jung *et al.*¹⁸ The article indicated that the physical properties of the hybrid materials were enhanced by the introduction of amine POSS. With the increasing content of POSS, better thermal properties and lower dielectric constants were obtained. And many other POSS/PI hybrid materials used in integrated circuits industry were also reported.^{19–21} These hybrid materials met the demand of high-performance low dielectric constant PIs to a degree.

However, traditional POSS/PI films had much higher CTE values in the film plane direction ranging about 40–50 ppm/K than those of conductive layers (such as, 17 ppm/K for copper foil, 24 ppm/K for aluminum foil). This meant that, when PI films were formed on a metal substrate via thermal imidization after the solution casting of PAA, the PI/metal laminates underwent thermal stress arising from the CTE mismatch during the

Table I. The Feed Ratio of PAA with Different Chain Lengths

	m_{BPDA}/g	m_{ODA}/g	m_{BAPPO}/g	V_{DMAc}/mL
PAA-00 ^a	2.3538	1.4238	0	20
PAA-05	2.3538	1.3695	0.111	20
PAA-10	2.3538	1.2875	0.222	20
PAA-15	2.3538	1.2254	0.333	20
PAA-20	2.3538	1.1533	0.444	20

^aReference POSS/PI hybrid material without PPO-structure.

cooling process from cure temperature to room temperature. Consequently, it caused serious problems such as curling, cracking, and detaching of PI films. Therefore, considerable efforts had been made to decrease the CTEs of PIs. Systematic researches on the structure-CTE relationship in various aromatic PI systems revealed that low-CTE PIs (temporary < 20 ppm/K) had rigid PI chain backbones and electron-drawing groups in the chain backbones.^{22,23} Phenyl phosphine oxide (PPO) was known to be very good in enhancing thermal properties as well as adhesive, mechanical properties, and fire retardancy.^{24,25} Moreover, the PPO had not only rigid chemical structure, but also a strong electron-withdrawing property. The introduction of PPO-structure into polymers can reduce the CTE of the polymers. In order to provide low CTE and preferable thermal properties, PPO-structure was introduced into POSS/PI to get novel phosphorus-containing organic–inorganic materials. The materials were designed to be used in a variety of electric, microelectronic devices, and integrated circuits industry.

In this study, a series of novel structural phosphorus-containing POSS/PI hybrid materials were synthesized via an efficient two-step room-temperature reaction. The thermal properties, dielectric properties, and CTE were also investigated. And the effect of the PPO-structure on the POSS/PI hybrid materials was discussed seriously.

EXPERIMENTAL

Materials

PPO was obtained from Aladdin Shanghai Development, China. Bis (4-aminophenoxy) phenyl phosphine oxide (BAPPO) was synthesized as reported previously.^{26,27} OAPS was provided by Hybrid Plastics, USA. 4,4'-diaminodiphenyl ether (ODA) and 3,3',4,4'-biphenyl tetracarboxylic dianhydride (BPDA) were supplied by TCI. Toluene and *N,N*-dimethylacetamide (DMAc) were supplied by Beijing Chemical Industry. All the other common reagents were reagent grade, obtained from commercial source, and used as received.

Characterization

IR spectra (KBr pellets or films) were conducted on a Nicolet Impact 410 Fourier transform infrared spectrometer (FTIR) at room temperature (25°C). Differential scanning calorimetry (DSC) analysis was performed using a Mettler Toledo DSC821^e instrument at a heating rate of 10°C/min in a nitrogen purge of 200 mL/min. Thermogravimetric analysis (TGA) was performed

using a PerkinElmer Pyris 1 TGA analyzer at a heating rate of 10°C/min in air purge of 100 mL/min. ¹H-NMR experiments were carried out on a Bruker 510 spectrometer (500 MHz for ¹H) using DMSO-*d*₆ and CDCl₃ as solvent. The gel permeation chromatography (GPC) analysis was carried with a Waters 410 instrument with *N,N*-Dimethylformamide as the eluent and polystyrene as the standard. The dielectric constants of the polymer films (coated with silver by a vacuum evaporation method) were obtained using Hewlett–Packard 4285A apparatus at room temperature and the frequency was 103–106 Hz. Thermomechanical analysis (TMA) was performed using Mettler Toledo TMA/SDTA 841^e.

Synthesis of BAPPO

The BAPPO was synthesized in two steps. First, triphenylphosphine oxide was taken in a round bottom flask equipped with nitrogen atmosphere and sulphuric acid was added to it. The reactant was dissolved and then the reaction system was cooled with an ice/salt bath. Fuming nitric acid was added dropwise. After that, the system was kept at room temperature for 8 h. The reaction mixture was hydrolyzed over ice. After the melting of ice, the mixture was extracted with chloroform and washed with aqueous sodium bicarbonate solution until neutral pH. The solvent was removed. The solid product bis(3-nitro-phenol)phenylphosphine oxide (BNPPO) was obtained. Then, BNPPO was refluxed with anhydrous powder tin(II) and fuming hydrochloric acid. The product was recrystallized from ethanol.^{26,27} The structure of BAPPO was confirmed by IR, ¹H-NMR spectroscopy. The characteristic bonds of amino groups appear at 3408 cm⁻¹, 3205 cm⁻¹, 1628 cm⁻¹. ¹H-NMR (DMSO-*d*₆, ppm): 5.35–5.46 (s, 4.0H), 6.56–6.7 (t, 2.0H), 6.7–6.8 (*m*, 2.0H), 6.8–6.9 (*m*, 2.0H), 7.05–7.2 (*m*, 2.0H), 7.46–7.61 (*m*, 5.0H).

Table II. The Feed Ratio of POSS/PI Hybrid Materials

	m_{OAPS}/g	m_{PAA}/g
PI-00	0.0675	1.8888
PI-05	0.0675	1.9172
PI-10	0.0675	1.9463
PI-15	0.0675	1.9561
PI-20	0.0675	1.9756

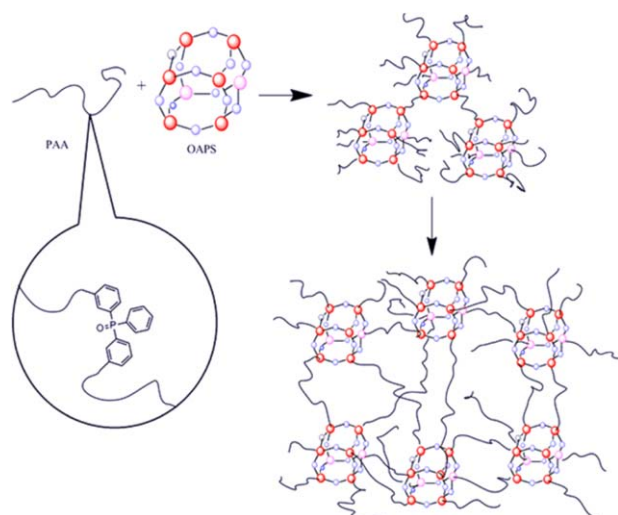


Figure 1. Synthesis route and suggested chemical structure of POSS/PI hybrid materials. [Color figure can be viewed in the online issue, which is available at wileyonlinelibrary.com.]

Synthesis of Phosphorus-Containing PAAs

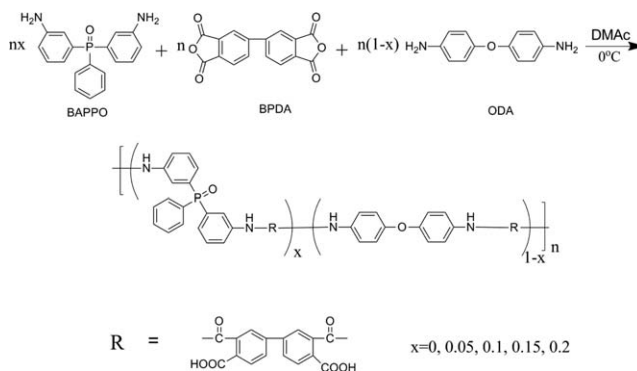
A series of phosphorus-containing polyamide acids were synthesized (Scheme 1). The ODA (1.153 g, 5.76 mmol), BAPPO (0.444 g, 1.44 mmol), BPDA (2.3538 g, 8.0 mmol) and DMAc (20 mL) were placed in a 50-mL two-necked round-bottom flask equipped with a mechanical stirrer under an argon stream. The solution was stirred for 8 h at 0°C to obtain the PAA20 (The content of the BAPPO in the diamines was 20%).

All the other PAAs were synthesized in a similar procedure and the feed ratios were shown in Table I. All the PAAs were washed ethanol and dried under vacuum.

Synthesis of POSS/PI Hybrid Materials

In a 100-mL two-neck round-bottom flask equipped with a mechanical stirrer and a condenser, PAA-20, OAPS, and DMAc were added. The reaction continued for 12 h at room temperature under an argon stream. Then the solution was coated on a glass plate by using an automatic film applicator and heated at 60, 80, 100, 120, 150, 200, 250, and 300°C in a nitrogen atmosphere for thermal imidization. The film of PI-20 which was synthesized with PAA-20 and OAPS was obtained.

All other films (PI-00, PI-05, PI-10, PI-15) were obtained using the similar synthetic routines and the feed ratio was shown in Table II. The synthesis route and suggested chemical structure of POSS/PI hybrid materials was shown in the Figure 1. As the



Scheme 1. Synthesis route and suggested chemical structure of phosphorus-containing PAAs.

figure showed, the three-dimensional chemical networks materials were expected.

RESULTS AND DISCUSSION

Synthesis of the POSS/PI Hybrid Materials

In order to study the effect of the PPO-structure on the POSS/PI hybrid materials, a series of polyimides were synthesized. First, a series of phosphorus-containing PAA were synthesized with BAPPO, ODA and BPDA. Excess BPDA was initially reacted with ODA and BAPPO. Anhydride groups were controlled as the terminal of the phosphorus-containing PAAs to facilitate their reaction with OAPS. The number-average molecular weight and weight-average molecular weight of the PAAs were obtained by GPC, as shown in Table III. The GPC results exhibited that a series of PAAs, whose length of the molecular chains was 19, were obtained.

Then, the POSS/PI hybrid materials were synthesized with OAPS and PAAs. However, this reaction was a typical $A_2 + B_8$ reaction, of which PAA was A_2 and OAPS was B_8 . Gelation easily occurred if the ratio was located in the gelation scope according to the Flory gelation theory.^{28–30} Thus, the key to copolymerization was to establish a suitable ratio of the terminal anhydride of the PAAs to the amine group of the POSS. Calculated and experimental results showed that the molar ratio was 7 : 1. The network-structured phosphorus-containing POSS/PI hybrid materials were synthesized. To obtain excellent phosphorus-containing POSS/PI hybrid materials, the controllability of temperature programming was essential.

Characterization of the POSS/PI Hybrid Materials

The FTIR spectra of the typical hybrid materials (PI-05 and PI-20) were shown in Figure 2. In the polyimides, a sharp and

Table III. The Molecular Weight of PAA

	m_{BPDA}/g	m_{ODA}/g	m_{BAPPO}/g	M_n	M_w	M_w/M_n
PAA-00	2.3538	1.4238	0	4654	6329	1.36
PAA-05	2.3538	1.3695	0.111	4635	5376	1.16
PAA-10	2.3538	1.2875	0.222	4857	6362	1.31
PAA-15	2.3538	1.2254	0.333	4870	6233	1.28
PAA-20	2.3538	1.1533	0.444	4719	5510	1.17

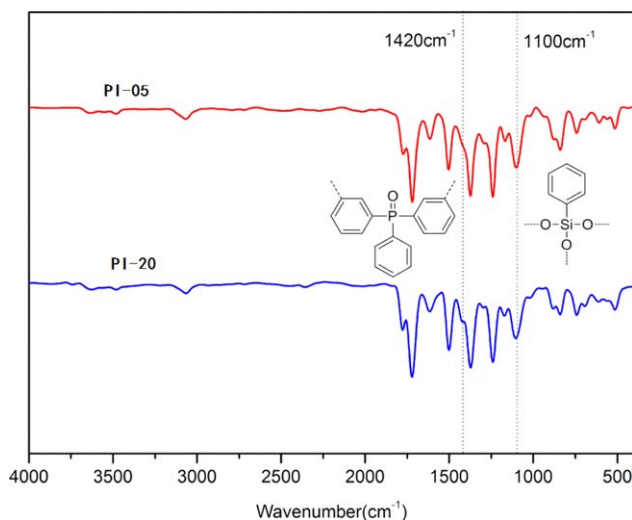


Figure 2. FTIR spectrum of the PI05 and PI20. [Color figure can be viewed in the online issue, which is available at wileyonlinelibrary.com.]

strong peak attributed to the Si—O—Si stretching of the silsesquioxane cage appeared at 1100 cm^{-1} . The characteristic imide group bonds at 1770 , 1710 , and 1380 cm^{-1} completely disappeared, which implied a fully imidized structure. The polyimide-derived C=C aromatic ring absorption at 1500 cm^{-1} was observed. Aromatic ether C—O—C stretching vibration was found at 1245 cm^{-1} . Ph—P appeared at 1420 cm^{-1} . The peak became stronger with the increasing of phosphorus content, which confirmed that a phosphonate structure existed in POSS/PI hybrid materials.

Thermal Properties of the POSS/PI Hybrid Materials

The DSC thermograms of POSS/PI hybrid materials were shown in Figure 3, respectively. Furthermore, a summary of the thermograms was given in Table IV. With the content of BAPPO increasing, the value of T_g raised to 301°C from 271°C . The T_g of POSS/PI hybrid materials was raised by the incorporation of PPO-structure into polymer matrix. With the introduction of PPO-structure in chains of polyimides, the C electron cloud density and intermolecular forces increased because of the P=O bond, which provided the electronic properties that resulted in the difficulty of segmental motion and increased T_g . And rigid PPO-structures would greatly inhibit the movement of segments of polyimides, thus also leading to a higher value of T_g .

Table IV. Thermal and Dielectric Properties of POSS/PI Hybrid Materials

	BAPPO content ^a	T_g ($^\circ\text{C}$)	$T_{d5\%}$ ($^\circ\text{C}$)	$T_{d10\%}$ ($^\circ\text{C}$)	Dielectric constant (κ) (at 1 MHz)	CTE (ppm/K)
PI-00	0	1.8888	470	509	3.39	46.31
PI-05	5%	1.9172	481	523	3.11	36.17
PI-10	10%	1.9463	502	560	2.90	33.71
PI-15	15%	1.9561	512	566	2.80	31.31
PI-20	20%	1.9756	580	602	2.64	27.45

^aThe molar quantities of BAPPO: the molar quantities of diamines.

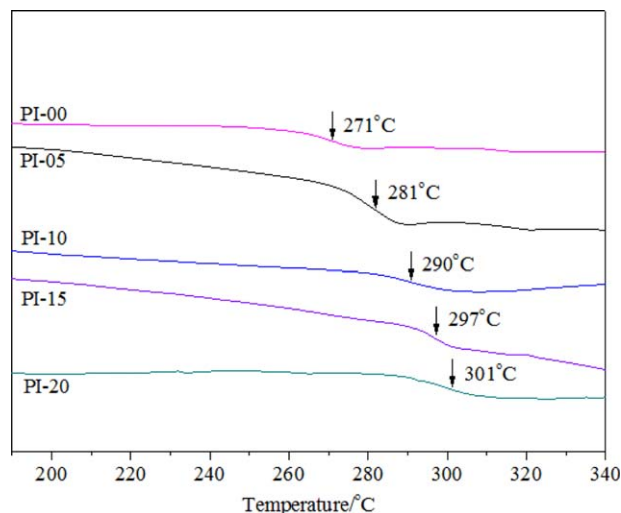


Figure 3. The DSC curves of the POSS/PI hybrid materials. [Color figure can be viewed in the online issue, which is available at wileyonlinelibrary.com.]

The thermal stability of the POSS/PI hybrid materials was evaluated using TGA in atmosphere and the TGA curves were shown in Figure 4. An evident increase in both 5% T_d and 10% T_d was observed for the phosphorus-containing POSS/PI hybrid materials compared with the reference POSS/PI. This phenomenon was due to the P=O with high bond energy, which resulted in higher degradation temperature.^{31–33} The phosphorus-containing POSS/PI hybrid materials displayed higher residuals of degradation than reference POSS/PI, and the yields of the degradation residues increased as the PPO-structure content increased. The original yield of degradation residue was ascribed to the ceramic formation from POSS moiety during thermal decomposition. And the increased yields of degradation residues were ascribed to phosphorus oxide.

The Dielectric Properties of POSS/PI Hybrid Materials

The dielectric properties were investigated by Hewlett–Packard 4285A apparatus. Figure 5 presented the dielectric constants (κ) of POSS/PI hybrid materials at a frequency ranging from 1000 Hz to 1 MHz. The dielectric constants (κ) of POSS/PI hybrid materials at 1 MHz were shown in Table IV. It was shown that the dielectric constants of the phosphorus-containing POSS/PI hybrids polymers ($\kappa = 3.11$ – 2.64 at 1 MHz) were lower than that of reference POSS/PI ($\kappa = 3.39$) under the same test condition. Moreover, the dielectric contents of polymers decreased

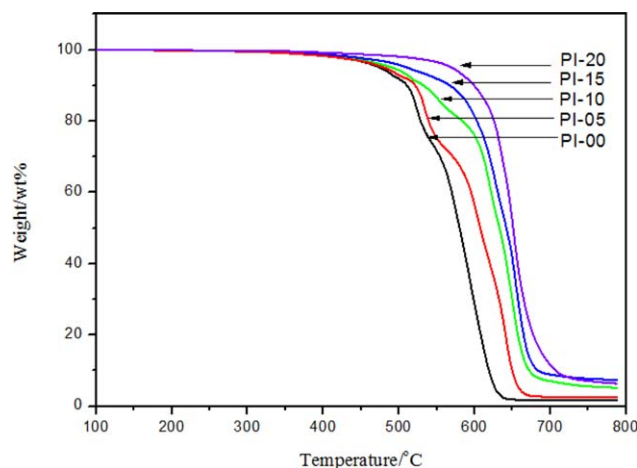


Figure 4. The TGA curves of the POSS/PI hybrid materials. [Color figure can be viewed in the online issue, which is available at wileyonlinelibrary.com.]

with the content of PPO-structures increasing. PPO-structures in the polyimide backbone was known to provide noncoplanar structure and big side groups, which can reduce the packing density of the chains. The introduction of PPO-structure maybe led to a lower packing density of chains and thereby reducing the dielectric contents.

Thermal Mechanical Properties of POSS/PI Hybrid Materials

The CTE values of POSS/PI hybrid materials (15 mm long, 5 mm wide, and 20 μm thick) in the glassy region were measured as an average within 100–250°C for the film plane direction by TMA at a heating rate of 10 K/min on a thermomechanical analyzer with a load (0.5 g per a unit film thickness in 1 μm , namely, 10 g load for 20 μm thick film) in a nitrogen flow. The TMA curves of the POSS/PI hybrid materials were shown in in Figure 6. The CTEs calculated from the film's dimension change during thermal ramping from 100 to 250°C are shown in Table IV. With the increase in BAPPO content, CTE decreased to 27.45 (ppm/K) from the value 46.31 (ppm/K) of reference POSS/PI. It was known that CTE depended crit-

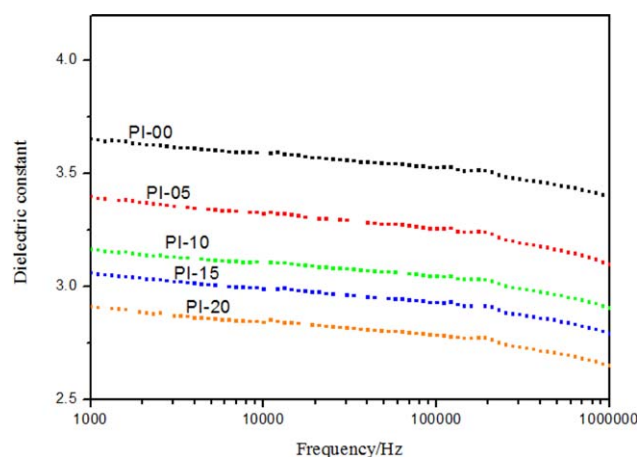


Figure 5. Frequency dependence of dielectric constants of POSS/PI hybrid materials. [Color figure can be viewed in the online issue, which is available at wileyonlinelibrary.com.]

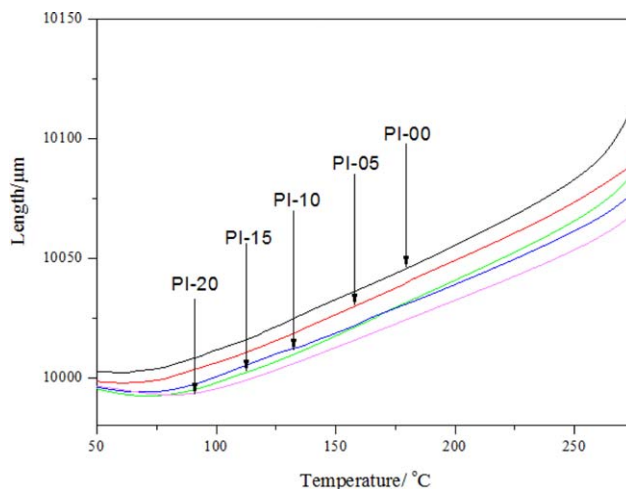


Figure 6. The TMA curve of the POSS/PI hybrid materials. [Color figure can be viewed in the online issue, which is available at wileyonlinelibrary.com.]

ically on molecular bond structures, such as monomer rigidity and chains mobility.¹⁸ The PPO-structure had not only rigid chemical structure, but also a strong electron-withdrawing property which can reduce the chains mobility of polymer. Among POSS/PI hybrid materials, as was expected, BAPPO played a much positive role in reducing CTE.

CONCLUSIONS

In this article, a series of novel structural phosphorus-containing POSS/PI hybrid materials, which incorporated PPO-structure into the main chains of POSS/PI, were prepared. The structures of the POSS/PI hybrid materials were characterized via FTIR spectroscopy. The DSC data showed that the T_g of the POSS/PI hybrid materials increased significantly with increasing PPO-structure content. The TGA data indicated that the stability of the POSS/PI hybrid materials was markedly improved in terms of T_{d5} and the yields of degradation residues. Besides, PPO-structure also contributed to low dielectric contents in a degree. Finally, the CTEs were measured and the results indicated that the introduction of PPO-structure into POSS/PI hybrid materials can reduce CTE markedly.

ACKNOWLEDGMENTS

The authors are grateful to Graduate Innovation Fund of Jilin University for financial support.

REFERENCES

1. Volksen, W.; Miller, R. D.; Dubois, G. *Chem. Rev.* **2010**, *110*, 56.
2. Matsui, S.; Sato, H.; Nakagawa, T. *J. Membr. Sci.* **1998**, *141*, 31.
3. Wang, P. J.; Lin, C. H.; Chang, S. L.; Shih, S. J. *Polym. Chem.* **2012**, *3*, 2867.
4. Tian, G.; Qi, S.; Chen, F.; Shi, L.; Hu, W.; Wu, D. *Appl. Phys. Lett.* **2011**, *98*, 203302.

5. Ji, D.; Jiang, L.; Cai, X.; Dong, H.; Meng, Q.; Tian, G.; Wu, D.; Li, J.; Hu, W. *Org. Electron.* **2013**, *14*, 2528.
6. Li, T.; Hsu, S. L. *J. Mater. Chem.* **2010**, *20*, 1964.
7. Ghosh, A.; Kumar, S. S.; Banerjee, S.; Voit, B. *RSC Adv.* **2012**, *2*, 5900.
8. Baskaran, S.; Liu, J.; Domansky, K.; Kohler, N.; Li, X.; Coyle, C.; Fryxell, G. E.; Thevuthasan, S.; Williford, R. E. *Adv. Mater.* **2000**, *12*, 291.
9. Maier, G. *Prog. Polym. Sci.* **2001**, *26*, 3.
10. Bosman, A. W.; Sijbesma, R. P.; Meijer, E. W. *Mater. Today* **2004**, *7*, 34.
11. Connell, J. W.; Watson, K. A. *High Perform. Polym.* **2001**, *13*, 23.
12. Verker, R.; Grossman, E.; Gouzman, I.; Eliaz, N. *Polymer* **2007**, *48*, 19.
13. Tanaka, K.; Chujo, Y. *J. Mater. Chem.* **2012**, *22*, 1733.
14. Leu, C. M.; Reddy, G. M.; Wei, K. H.; Shu, C. F. *Chem. Mater.* **2003**, *15*, 2261.
15. Kannan, R. Y.; Salacinski, H. J.; Butler, P. E.; Speifalian, A. M. *Acc. Chem. Res.* **2005**, *38*, 879.
16. Zhang, C.; Laine, R. M. *J. Am. Chem. Soc.* **2000**, *122*, 6979.
17. Geng, Z.; Huo, M. *J. Mater. Chem. C* **2014**, *2*, 1094.
18. Youngsuk, J.; Sunjung, B.; Sungjun, P.; Hyunmi, L. *Appl. Mater. Interfaces* **2014**, *6*, 6054.
19. Liao, W. H.; Yang, S. Y.; Hsiao, S. T. *Appl. Mater. Interfaces* **2014**, *6*, 15802.
20. Verker, R.; Grossman, E.; Eliaz, N. *Compos. Sci. Technol.* **2012**, *72*, 1408.
21. Verker, R.; Grossman, E.; Gouzman, I.; Eliaz, N. *Compos. Sci. Technol.* **2009**, *69*, 2178.
22. Numata, S.; Oohara, S.; Fujisaki, K.; Imaizumi, K.; Kinjyo, N. *J. Appl. Polym. Sci.* **1986**, *31*, 101.
23. Numata, S.; Fujisaki, K.; Kinjyo, N. *Polymer* **1987**, *28*, 2282.
24. Martinez-Nunez, M. F.; Sekharipuram, V. N.; McGrath, J. E. *Polym. Prepr.* **1994**, *35*, 709.
25. Lee, Y. J.; Gungor, A.; Yoon, T. H.; McGrath, J. E. *J. Adhesion* **1995**, *55*, 165.
26. Liu, Y.; Hsiue, G.; Lee, R. *J. Appl. Polym. Sci.* **1997**, *63*, 895.
27. Meenakshi, K. S.; Sudhan, E. P. *J. Appl. Nanosci.* **2011**, *1*, 109.
28. Stockmayer, W. H. *J. Chem. Phys.* **1943**, *11*, 45.
29. Stockmayer, W. H.; Casassa, E. F. *J. Chem. Phys.* **1952**, *20*, 1560.
30. Xu, N.; Stark, E. J.; Dvornic, P. R.; Meier, D. J.; Hu, J.; Hartmann-Thompson, C. *Macromolecules* **2012**, *45*, 4730.
31. Lin, C. H.; Wu, C. Y.; Wang, C. S. *J. Appl. Polym. Sci.* **2000**, *78*, 228.
32. Lin, C. H.; Chang, S. L.; Wei, T. P.; Ding, S. H.; Su, W. C. *Polym. Degrad. Stab.* **2010**, *95*, 1167.
33. Chang, H. C.; Lin, H. T.; Lin, C. H. *Polym. Chem.* **2012**, *3*, 970.